Partitioning of Differently Sized Poly(ethylene glycol)s into OmpF Porin

Tatiana K. Rostovtseva,*† Ekaterina M. Nestorovich,* and Sergey M. Bezrukov*‡

*Laboratory of Physical and Structural Biology, National Institute of Child Health and Human Development, National Institutes of Health, Bethesda, Maryland 20892-0924 USA; †Department of Biology, University of Maryland, College Park, Maryland 20742 USA; and ‡St. Petersburg Nuclear Physics Institute, Gatchina 188350, Russia

ABSTRACT To understand the physics of polymer equilibrium and dynamics in the confines of ion channel pores, we study partitioning of poly(ethylene glycol)s (PEGs) of different molecular weights into the bacterial porin, OmpF. Thermodynamic and kinetic parameters of partitioning are deduced from the effects of polymer addition on ion currents through single OmpF channels reconstituted into planar lipid bilayer membranes. The equilibrium partition coefficient is inferred from the average reduction of channel conductance in the presence of PEG; rates of polymer exchange between the pore and the bulk are estimated from PEG-induced conductance noise. Partition coefficient as a function of polymer weight is best fitted by a "compressed exponential" with the compression factor of 1.65. This finding demonstrates that PEG partitioning into the OmpF channel pore has sharper dependence on polymer molecular weight than predictions of hard-sphere, random-flight, or scaling models. A 1360-Da polymer separates regimes of partitioning and exclusion. Comparison of its characteristic size with the size of a 2200-Da polymer previously found to separate these regimes for the α-toxin shows good agreement with the x-ray structural data for these channels. The PEG-induced conductance noise is compatible with the polymer mobility reduced inside the OmpF pore by an order of magnitude relatively to its value in bulk solution.

INTRODUCTION

Water-soluble polymers are widely used to probe ion channel structures in their functional states (Zimmerberg and Parsegian, 1986; Krasilnikov et al., 1992, 1998; Bezrukov and Vodyanoy, 1993; Bezrukov et al., 1994, 1996; Parsegian et al., 1995; Villarroel et al., 1995; Bullock and Kolen, 1995; Korchev et al., 1995; Bezrukov and Kasianowicz, 1997, 2001; Desai and Rosenberg, 1997; Kaulin et al., 1998; Ternovsky and Berestovsky, 1998; Merzlyak et al., 1999; Howorka et al., 2000; Krasilnikov, 2001; Movileanu et al., 2001). Polymer addition changes solution properties that modify channel behavior. In particular, neutral polymers decrease the specific solution conductivity and interfere with ionic flow through the channel in a manner that depends on polymer molecular weight. They also exert osmotic stress on the structures that have polymer-inaccessible water cavities, e.g., channel pores in the presence of sterically excluded polymers. The methods of polymer probing have been mostly applied to ion channels whose water-filled pores are 1 nm or larger in diameter. In the presence of differently sized polymers the ionic conductance of these large channels demonstrates well-defined transitions between regimes of polymer penetration and exclusion.

Here we use water-soluble polymers to probe the OmpF porin channels. OmpF porin is one of the major outer membrane proteins of *Escherichia coli* (Nikaido and Vaara, 1985). The 3D structure of OmpF is visualized with high resolution (Cowan et al., 1992). The channel comprises three monomers; each monomer forms a 16-stranded β-barrel, which serves as a water-filled pore. The transmembrane length of the inner barrel wall is ~3.0 nm, which is less than the thickness of the lipid bilayer. The barrel has an elliptical cross-section of 2.7×3.8 nm between main-chain atoms in the barrel walls. Within each monomeric pore a polypeptide loop is bent into the channel and, at a height corresponding to the center of the pore, constricts the pore considerably (Cowan et al., 1992; Cowan, 1993; Lou et al., 1996; Dutzler et al., 1999). The crystal structure shows the dimensions of the narrowest part being 0.7×1.1 nm. The pore diameter increases abruptly just beyond the constriction zone.

When reconstituted into the bilayer lipid membranes, OmpF porin forms large, slightly cation-selective channels (Benz et al., 1978, 1979, 1985; Schindler and Rosenbusch, 1978; Engel et al., 1985; Buehler et al., 1991; Saint et al., 1996). It has been shown that high applied voltages (130–200 mV) cause the closure of OmpF monomers, so that the porin-induced conductance decreases the open channel conductance in steps of approximately one-third (Engel et al., 1985). The monomer closure is a reversible process.

Solute exclusion experiments have been used to evaluate the size of the pore. Liposome studies showed that the upper molecular weight of solutes able to pass through the OmpF pores falls into a range of 500–700 (Decad and Nikaido, 1976; Nakae, 1976a, b). The raffinose was used to estimate the pore diameter of 1.13 nm (Douglas et al., 1984). A diameter of 1.0–1.2 nm for OmpF pore was proposed, based on permeability rates (Nikaido and Rosenberg, 1983).

One could argue that once the crystal structure of general porins has been resolved, there is no need to assess the pore size by alternative methods. Although this is true if one assumes that the crystallographic structure represents the functional channel in its open conformation, the transport

Received for publication 26 June 2001 and in final form 29 August 2001.

Address reprint requests to Dr. Sergey M. Bezrukov, NIH, Bldg. 9, Room 1E-122, Bethesda, MD 20892-0924. Tel.: 301-402-4701; Fax: 301-402-9462; E-mail: bezrukov@helix.nih.gov.

0006-3495/02/01/160/10 $2.00

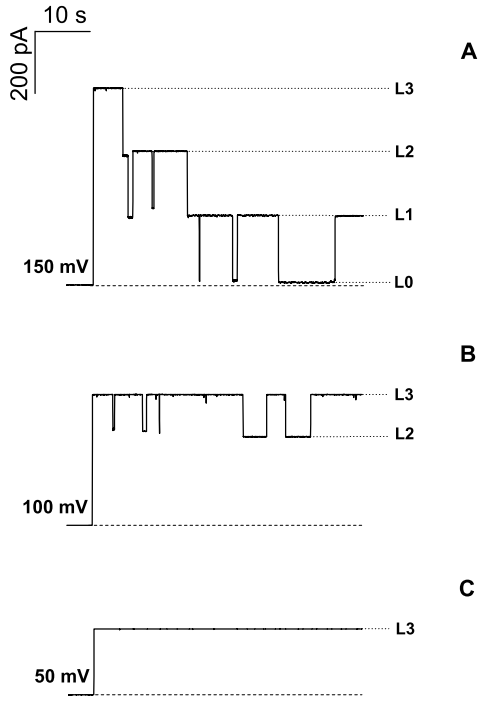

FIGURE 1 Typical recordings of ion currents through single trimeric OmpF channels reconstituted into planar lipid bilayer membranes at 150 mV (*A*), 100 mV (*B*), and 50 mV (*C*) show that channel stability depends on the applied voltage. Large voltages close the channel in three approximately equal steps, revealing its trimeric organization. Dotted lines L3, L2, L1, and L0 correspond to fully open, one-monomer closed, two-monomer closed, and three-monomer closed states, correspondingly. The dashed line shows zero-current level. The membrane-bathing solution contained 1 M KCl, 1 mM $CaCl_2$, and 5 mM HEPES at pH 7.0. Time resolution was 10 ms.

properties of the channel for different solutes are not defined by the pore geometry alone. In addition to purely steric repulsion, a number of complex interactions have to be considered to understand quantitative features of transport. In what follows we study the dynamic partitioning of differently sized neutral polymers, poly(ethylene glycol)s (PEGs), between the bathing solution and the pore by observing the behavior of a single OmpF channel in their presence.

We deduce both partitioning equilibria and partitioning kinetics using polymer-induced changes in the current through a single channel formed by the OmpF trimer in a lipid bilayer membrane. This channel is well suited for studying polymer-pore interactions, because it can remain in the open state for an extended period of time (Fig. 1). We use the changes in the mean current through the channel to estimate polymer partition coefficient and polymer-induced current fluctuations to determine polymer mobility within the pore. We compare the OmpF results with previously obtained data for polymers partitioning into the alamethicin and α-toxin channels, and discuss our main findings using known crystallographic data for α-toxin and OmpF channels.

We show that mobility of PEG in the OmpF pore is comparable to its mobility in alamethicin channels (Bezrukov et al., 1994) that do not exhibit any attractive interactions with PEG. Comparison with the α-toxin channel demonstrates that the characteristic molecular weights of polymers that separate regimes of polymer exclusion and penetration are in accord with x-ray data. That is, the ratio of average effective radii of α-toxin and OmpF pores calculated from crystallographic structures is $\sim$1.4; the ratio of corresponding polymer hydrodynamic radii is 1.3.

Although probing ion channels with water-soluble polymers is a useful practical method for studying pore geometry in a functional state, the physics of polymer partitioning in the confines of the channel pore is not well understood. More theoretical and experimental work is needed to develop the full potential of the method of polymer probing and to understand the main principles of channel-facilitated transport of long, flexible molecules.

MATERIALS AND METHODS

OmpF was a generous gift of Dr. Mathias Winterhalter. Bilayer membranes were formed from monolayers made from a 1% solution of diphytanoylphosphatidylcholine (Avanti Polar Lipids, Inc., Alabaster, AL) in hexane (Aldrich Chemical Co., Inc., Milwaukee, WI) or pentane (Burdick and Jackson, Muskegon, MI) on 70–80-μm diameter orifices in the 15-μm-thick Teflon partition that separated two chambers (after Montal and Mueller, 1972). The orifices were pretreated with a 1% solution of hexadecane in pentane. The total capacitance was $\sim$70 pF and the film capacitance was 30–35 pF. Aqueous solutions of 1 M KCl containing 1 mM $CaCl_2$ were buffered by 5 mM MES at pH 4.6 or HEPES at pH 7.0. All measurements were made at room temperature (23.0 $\pm$ 1.5)°C.

Single-channel insertion was achieved by adding 0.1–0.3 μl of a 1 μg/ml solution of OmpF in the buffer that contained 1 M KCl and 1% (v/v) of Octyl POE (Alexis, Switzerland)) to 1 ml aqueous phase at one side of the membrane only while stirring at 100 mV applied voltage. After a single channel was inserted and its parameters were recorded, membrane-bathing solutions in both compartments were perfused with 15% (w/w) solutions of differently sized PEGs (Aldrich Chemical Co.). To keep the ion/water molar ratio constant, the polymers were added to 1 M KCl stock solutions. At the end of each experiment we checked the quality of perfusion. The contents of both compartments were taken to measure conductivity using a CDM 83 conductivity meter (Radiometer, Copenhagen, Denmark) to determine the actual polymer concentrations in the experimental cell.

The membrane potential was applied using Ag/AgCl electrodes in 3 M KCl, 15% agarose bridges assembled within standard 200 μl pipette tips (Bezrukov and Vodyanoy, 1993). Potential is defined as positive when it is greater at the side of protein addition. The current was amplified by a Dagan 3900 integrating patch-clamp amplifier (Dagan Corp., Minneapolis, MN) with a 3902 headstage or by an Axopatch 200B amplifier (Axon Instruments, Inc., Foster City, CA) in the voltage clamp mode. Data were filtered by a low-pass 8-pole Butterworth filter (Model 9002, Frequency Devices, Inc., Haverhill, MA) at 15 kHz and recorded simultaneously by a VCR operated in a digital mode, and directly saved into the computer memory with a sampling frequency of 50 kHz. Amplitude and power spectrum analysis was done using software developed in-house. The membrane chamber and headstages were isolated from external noise sources with a double metal screen (Amuneal Manufacturing Corp., Philadelphia, PA).

RESULTS

Addition of OmpF porin to the membrane-bathing aqueous phase caused the stepwise current increase that corresponded to the opening of a single trimeric channel. At neutral pH and applied potential <100 mV, the spontaneous channel closure was rare. Channels were stable for extended periods and showed rather low open channel noise. However <5.0, channels were less stable and it was possible to observe their closures within several minutes already at 100 mV. Therefore, to resolve the trimeric structure of OmpF channel and to obtain data on individual monomers, we performed some of our experiments at pH 4.6.

Fig. 1 *A* illustrates typical current steps generated by a single OmpF channel at 150 mV with total (integral) conductance of 4.3 nS. The process of channel closure under applied voltage is seen as a stepwise reduction in conductance, most likely representing sequential monomer closures. Changes in conductance upon transitions between levels L1, L2, and L3 are somewhat smaller than one-third of the total channel conductance. The actual conductances of individual monomers must include parts of the residual conductance represented by L0 (see also Schindler and Rosenbusch, 1978). The levels had very close, but usually not identical, amplitudes. The "closed level," L0, was least reproducible, giving the largest relative spread of conductance (0.24 ± 0.12) nS. We never observed an OmpF channel that would close to zero current (corresponding to the membrane leakage of $\sim$0.5 pA); however, the amplitude of level L0 was quite variable even within an experiment with the same channel.

Fig. 1, *B* and *C* show that at smaller voltages the channel is more stable. At pH 7.0 and 100 mV of applied voltage the channel spontaneously "gates" to $\sim$⅔ of its initial conductance. At 50 mV the channel stays in the completely open conformation for extended periods of time. In 1 M KCl the channel is rather ohmic in the range of $\pm$200 mV, with only a slight monotonic decrease in conductance with the increase in applied potential, reaching $\sim$6% at $+$200 mV.

Addition of polymers changes channel conductance. The magnitude of this change depends on polymer molecular weight. Fig. 2 illustrates the effect of perfusion of polymer-free membrane-bathing solution with solutions containing 15% PEG. All three current records represent a completely open channel (level L3). Similar relative changes were found for levels L1 and L2 (corresponding records are not shown). It is seen that the large, presumably excluded PEG 10,000 practically does not change the ionic current through the channel. Smaller polymers, PEG 1000 and PEG 200, reduce channel conductance. In the presence of PEG 200, channel conductance is $\sim$0.65 of its value in polymer-free solution.

The relative polymer-induced reduction of channel conductance was found to be similar for all three monomers. Data in Fig. 3 obtained for PEG 1000 in experiments at pH

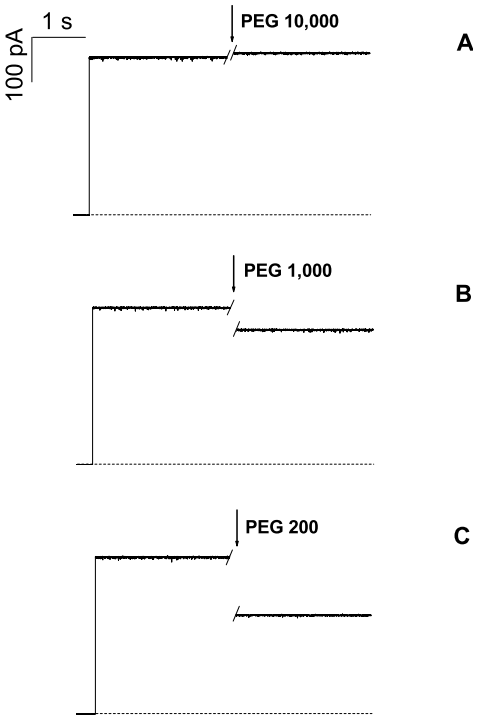

FIGURE 2 Effect of polymer addition on channel ion current depends on polymer molecular weight. Large polymers, such as PEG 10,000 (*A*), do not change the current appreciably. Smaller polymers, PEG 1000 (*B*) and PEG 200 (*C*), decrease channel conductance in a molecular weight-dependent manner. Monomeric concentration of polymer in the bulk was the same in all experiments and corresponded to 15% (w/w) PEG solutions. Applied voltage was 100 mV; pH 7.0; time resolution was 1 ms.

4.6, where the channel is more easily "gated" by voltage, illustrate this point. Within the experimental error all three conductance levels are changed by polymer addition in the same proportion. Indeed, level conductance is linear in level number both in the absence and in the presence of polymers. This suggests that polymers act on individual pores of the OmpF trimer independently. A similar observation was recently made for sugar partitioning into maltoporin channels (Bezrukov et al., 2000b). Thus, results obtained for the fully open channel are also characteristic for a single pore.

Fig. 4 summarizes conductance measurements for the range of PEG sizes used in the present study. Raw data (*filled squares*) are shown as ratios of the channel conductance in the presence of PEG to its conductance in polymer-free solution. It is seen that large polymers, i.e., with molecular weights 3400 and higher, do not change channel conductance appreciably, while smaller polymers decrease it significantly. PEGs with molecular weights of 400 and smaller decrease the channels conductance almost to the same extent as bulk solution conductivity (*dashed line*, corresponds to the 0.6 ± 0.02 drop in bulk conductivity measured by taking solutions from the cell compartments after the measurement was concluded).

Partitioning of polymers between the bulk and the channel pore usually generates measurable temporal fluc-

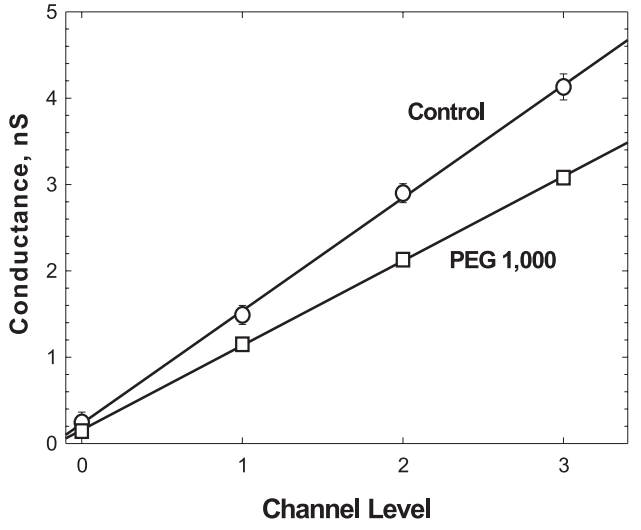

FIGURE 3 Within the experimental error, the effect of polymer addition scales with the level number, suggesting independent partitioning of PEG into individual monomeric pores. The relative polymer-induced conductance reduction is the same for the fully open channel, two open monomers, and only one open monomer. The solution contained 1 M KCl, 1 mM $CaCl_2$, and 5 mM MES at pH 4.6.

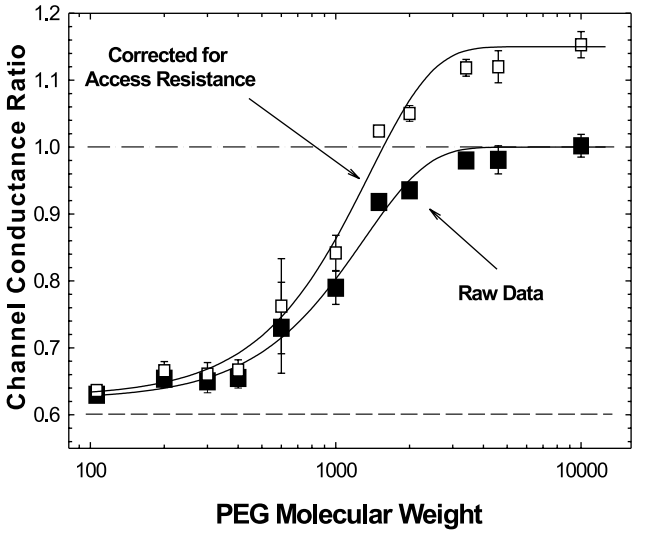

FIGURE 4 Conductance of the fully open OmpF channel in the presence of differently sized PEG normalized to its conductance in polymer-free solution is a function of polymer molecular weight (*filled squares*). All data points are averages for 50 and 100 mV of the applied voltage. Each point represents at least two different experiments where a single channel was first reconstituted and recorded in the polymer-free solution, which was then substituted by the polymer-containing one. The horizontal dashed line corresponds to PEG effect on the bulk solution. The bold line gives the best fit to Eqs. 1 and 2. Open squares and the thin solid line show the conductance ratio corrected for the channel access resistance. The solution contained 1 M KCl, 1 mM $CaCl_2$, and 5 mM HEPES at pH 7.0.

tuations in the channel conductance (Bezrukov et al., 1994, 1996). To obtain kinetic information on polymer partitioning, we analyzed the fragments of current recordings that were free from the fast stepwise closures evident at high time resolutions. These pH-dependent transients also exist in polymer-free solutions and will be investigated in our forthcoming paper. A more detailed description of the signal-selection procedure can be found elsewhere (Bezrukov et al., 1994; Bezrukov and Winterhalter, 2000). We quantify polymer-induced fluctuations in the OmpF channel by measuring the power spectral density of current noise in the presence of differently sized PEGs. Fig. 5 presents spectral densities of current fluctuations of the membrane containing a single OmpF trimer at zero voltage (1), at 100 mV in polymer-free solution (2), and at 100 mV in solution containing PEG 1000 (3). With the fragments of 10 s duration and the 24 Hz resolution bandwidth used in spectral analysis, the normalized standard error of spectral estimates is expected to be $(10 \times 24)^{-1/2}$, or ~6% for each point (Bendat and Piersol, 1986). It is seen that the difference between low-frequency parts of spectra (2) and (3) exceeds three standard errors.

The results for all PEGs used here are presented in Fig. 6 in the form of the low-frequency spectral density $S(0)$. It was obtained from the spectra, examples of which are given in Fig. 5, by averaging over the range 100 Hz $< f <$ 1000 Hz (where the PEG-induced component was "white") and by subtracting the background noise at 0 mV applied potential. Therefore, every point represents an average over 36 spectral estimates, so that the measurement error should further decrease by a factor of $(36)^{-1/2}$ to give the normalized standard error of ~1%. It is seen that error bars in Fig. 6 are at least an order of magnitude larger. These error bars reflect reproducibility of the PEG-induced noise from channel to channel rather than the limited statistics used for spectral estimates.

Comparison to alamethicin shows that, in the case of OmpF, the polymer-induced noise is small. It barely exceeds the background noise of the channel (*horizontal dotted line*) for the intermediately sized polymers and is even below the background noise for polymers of small size. The solid line represents a prediction for the noise of a channel in polymer-free solution, taking into account its polymer-reduced conductance (see below).

DISCUSSION

The similarity in the effect of PEG on different conducting levels of OmpF channel (Fig. 3) suggests that the channel is composed of three pores of almost uniform dimensions. This conjecture is in complete accord with the crystallographic data. Therefore, in our discussion we will use the data obtained for the OmpF trimer, that is, for the fully open channel, extending our main conclusions to each individual monomer. The exception is the closed state, L0 (Fig. 1) whose nature is not clear yet. The quantitative analysis of

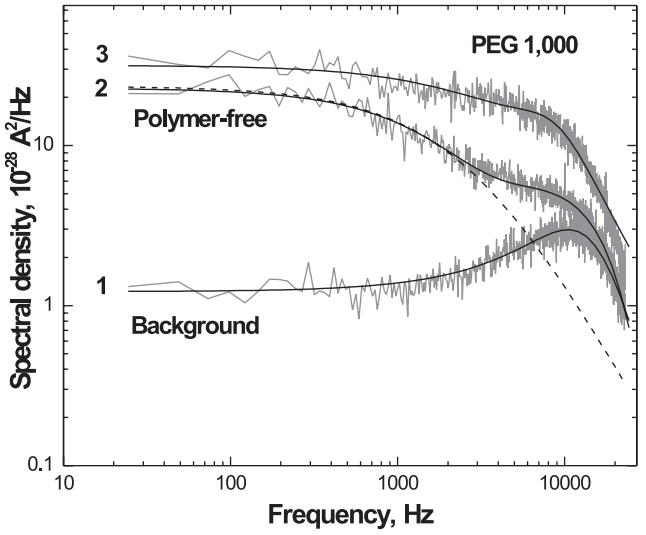

FIGURE 5 Power spectral density of noise in the ionic current through a single fully open channel is increased by addition of PEG 1000. At low frequencies ($f < 2$ kHz) the noise measured at zero applied voltage (*curve 1*) has an order of magnitude smaller values than the noise measured at 100 mV in polymer-free solution (*curve 2*) or polymer-containing solution (*curve 3*). The sharp cutoff starting at ~10,000 Hz is related to signal filtering. Already in the absence of polymer the low-frequency noise significantly exceeds both equilibrium and shot noise, and is described by a Lorentzian (*dashed line*) with a characteristic time of ~0.1 ms. We will address the origin of this noise in our forthcoming paper.

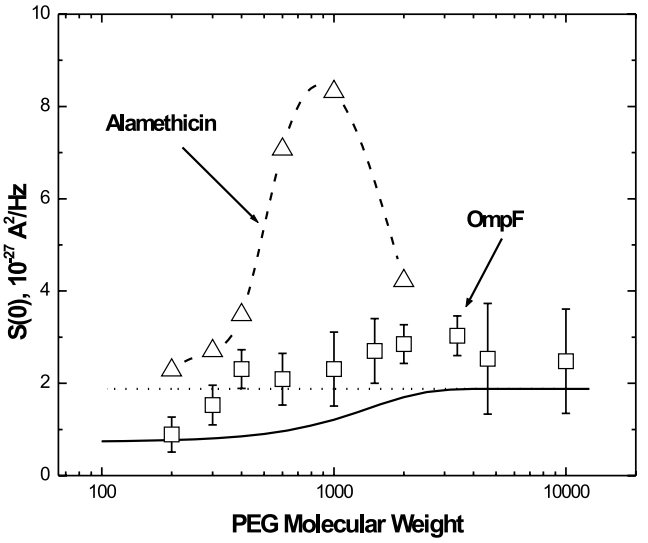

FIGURE 6 Addition of polymers induces excess noise in the ion current through the OmpF channel measured at 100 mV (*squares*), but the effect is not as expressed as in the case of alamethicin in state 3 (*triangles*, from Bezrukov et al., 1994). The horizontal dotted line represents open channel noise in polymer-free solution. The solid line is calculated to account for the polymer-induced decrease in channel conductance (see text).

this residual conductance is problematic due to the wide amplitude distribution of the level conductance obtained even for the same channel.

Partitioning equilibrium

Quantitative thermodynamic analysis of equilibrium polymer partitioning was performed for the α-hemolysin (α-toxin) channel (Bezrukov et al., 1996; Merzlyak et al., 1999) and, recently, for the alamethicin channel (Bezrukov and Kasianowicz, 2001) using previously published results (Bezrukov and Vodyanoy, 1993). To deduce partition coefficient from conductance data, a linear relationship between the polymer monomeric concentration in the pore and the reduction in the channel conductance is assumed. This assumption is based on two general observations. First, the PEG-induced decrease of the solution specific conductivity is not sensitive to the polymer molecular weight and is a fairly linear function of polymer monomeric concentration in the 0–15% range (Krasilnikov et al, 1992; Bezrukov and Vodyanoy, 1993; Parsegian et al., 1995; Berezhkovskii et al., 1999). Second, in the case of large channels, the effects of small polymers on the bulk solution conductivity and on the channel conductance are very close to each other. Thus, there is no reason to expect any significant non-linear corrections and, therefore, the relationship between channel conductance and polymer partition coefficient $p(w)$ can be expressed as:

$$g(w)/g(\infty) = 1 - \chi p(w) \quad (1)$$

where $g(w)$ is channel conductance in the presence of polymer with molecular weight w, $g(\infty)$ is channel conductance in the presence of completely excluded large polymer, and parameter χ describes the relative amplitude of the channel conductance change between the regimes of completely excluded and completely penetrating polymers (for more details see Bezrukov et al., 1996).

To compare polymer partitioning into the OmpF channel with earlier data for alamethicin and α-toxin channels, we use a simple scaling law

$$p(w) = \exp(-(w/w_0)^{\alpha}) \quad (2)$$

for the partitioning coefficient $p(w)$ with adjustable α and w_0. The first parameter characterizes the sharpness of transition between regimes of exclusion and penetration. Sharper transitions correspond to larger α values. The second parameter is the characteristic polymer molecular weight ("cutoff size") that separates these two regimes. The bold solid line in Fig. 4 represents the results of fitting that yield $w_0 = 1360$, $\alpha = 1.65$, and $\chi = 0.37$.

The characteristic molecular weight of 1360 corresponds to a PEG hydrodynamic radius of ~1.0 nm (Couper and Stepto, 1969; Kuga, 1981). The transition sharpness characterized by parameter α exceeds those predicted by the scaling approach (De Gennes, 1979; Grosberg and Khokhlov, 1994), hard sphere partitioning

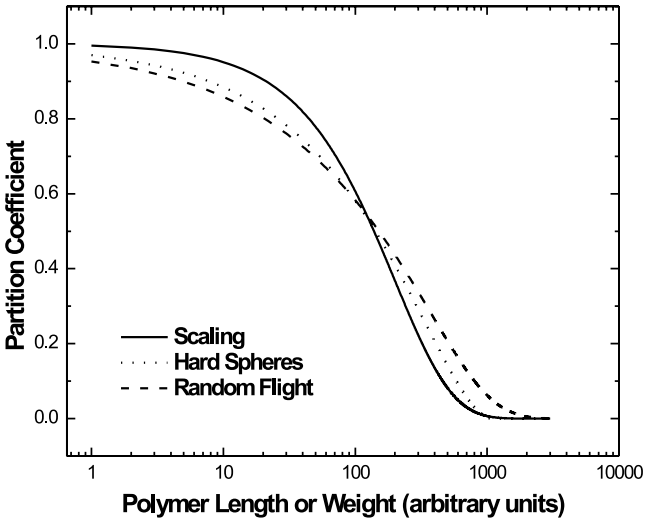

FIGURE 7 Comparison of three available theoretical models for partitioning, random flight (*dashed line*), hard spheres (*dotted line*), and scaling (*solid line*) shows that scaling arguments give the sharpest transition between penetration and exclusion. The "polymer weight" scale is adjusted to make all three curves to coincide at a partition coefficient equal to ½.

(e.g., Colton et al., 1975), or random flight model (Casassa, 1967). A comparison of these three models for polymer partitioning into long circular cylindrical channel of radius R is shown in Fig. 7 (see also Bezrukov and Kasianowicz, 2001). It can be seen that the scaling approach that is represented by

$$p^{sc}(w) = \exp(-w/w_{sc}) \tag{3}$$

where w_{sc} is not defined within the scaling arguments, gives the sharpest transition corresponding to $\alpha = 1.0$. Hard-sphere partitioning

$$p^{hs}(w) = \begin{cases} (1 - r_h(w)/R)^2 & \text{at} \quad r_h(w) \le R \\ 0 & \text{at} \quad r_h(w) > R \end{cases} \tag{4}$$

where the effective radius of the "hard-sphere polymer" $r_h(w)$ is assumed to scale as $w^{3/5}$, and partitioning given by the random-flight model (Casassa, 1967)

$$p^{rf}(w) = 4 \sum_{m=1}^{\infty} \frac{1}{\beta_m^2} \exp[-(\beta_m r_i(w)/R)^2], \tag{5}$$

where β_m are the roots of a zero-order Bessel function of the first kind and $r_i(w)$ scales as $w^{1/2}$, both give appreciably smoother transitions between partitioning and exclusion.

These three models are tempting to use because they give the closed-form analytical expressions for partition coefficient. Indeed, by applying them to our data we ignore several complications. One of them is the high polymer concentration used in our experiments. At 15% concentration the PEG 1000 solution is on the border between diluted and semi-diluted regimes, where interactions between polymer molecules can no longer be neglected. This problem was addressed earlier (Merzlyak et al., 1999) and it was shown that only the highly artificial hard-sphere model is able to give an appreciably sharper transition. Direct application of the scaling model is also questionable because it is formulated in the assumption of highly confined polymers, the assumption, which breaks for small PEGs used in our studies. The most appropriate model seems to be the random-flight model (Casassa, 1967), whose quantitative predictions are still used to estimate the effects of polymer confinement (e.g., Cifra and Bleha, 2001).

It is easy to demonstrate that corrections for the finite access resistance do not influence the transition sharpness and the characteristic "cutoff" polymer size significantly. Indeed, considering the access resistances at the both sides of the OmpF channel to be equal to one another and using methods described previously (Bezrukov and Vodyanoy, 1993), we can determine the ratio of channel conductances with the access contributions eliminated. The open squares in Fig. 4 show this conductance ratio calculated for each polymer concentration. It is seen that for large, completely excluded polymers the conductance of the channel corrected for the access resistance significantly exceeds its value in the absence of polymers. This polymer-induced conductance increase is explained by the increase in the salt ion activity upon PEG addition (Bezrukov and Vodyanoy, 1993). PEG binds water molecules and effectively increases salt concentration in polymer-free water cavities. The thin solid line in Fig. 4 is drawn according to Eqs. 1 and 2, with $g(w)$ and $g(\infty)$ now standing for the conductances of the channel with the access contributions eliminated. The corresponding partitioning parameters coincide within 3% with those for the bold curve. Total access resistance in polymer-free solution is calculated to be 3.9×10^7 Ohm; the corresponding effective radius of channel entrances is 1.2 nm.

Fig. 8 shows the comparison of PEG partitioning into the OmpF channel with partitioning into alamethicin (level 1) and α-toxin channels obtained in previous studies (Bezrukov and Vodyanoy, 1993; Bezrukov et al., 1994, 1996; Bezrukov and Kasianowicz, 2001). The lines are drawn according to Eq. 1, with $w_0 = 980$ and $\alpha = 1.3$ for alamethicin and $w_0 = 2200$ and $\alpha = 3.2$ for α-toxin channels. The curves are obtained for polymer partitioning at 15% (w/w) PEG dissolved in 1 M NaCl. To allow for polymer-channel attraction in the case of α-toxin, the partition coefficient scaling was assumed to have the form $1.1 \exp(-(w/w_0)^{\alpha})$. All three curves suggest that the channel radii increase in the sequence alamethicin $<$ OmpF $<$ α-toxin. They also show that the transition between penetration and exclusion regimes is sharper

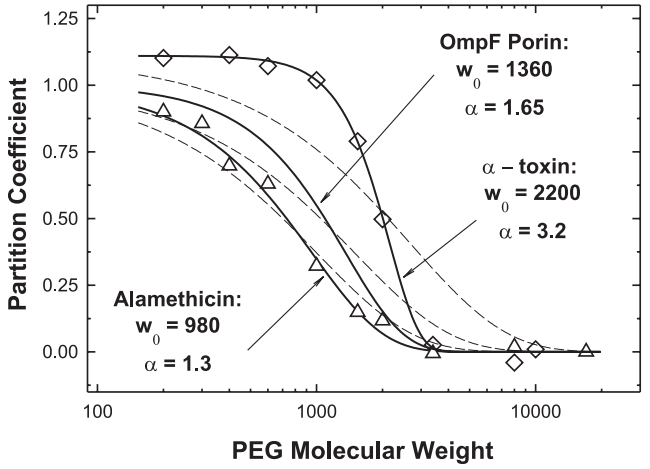

FIGURE 8 Polymer partitioning into alamethicin, OmpF porin, and α-toxin channels is described by "compressed exponents" with the compression factor ranging from 1.3 for alamethicin to 3.2 for α-toxin. All three curves demonstrate sharper dependencies of partitioning on polymer molecular weight than the three theoretical models for steric repulsion summarized in Fig. 7 predict. Dashed lines represent the best fit of the scaling theory.

($\alpha > 1.0$) than any of the theories summarized in Fig. 6 predict.

There are no reliable structural data on alamethicin channels (Sansom, 1991; Cafiso, 1994; Wallace, 2000). However, crystallographic structures of OmpF (Cowan et al., 1992) and α-toxin (Song et al., 1996) channels are available. We compare their pores in Fig. 9, where a monomer of OmpF is shown in gray and the outline of the water-filled

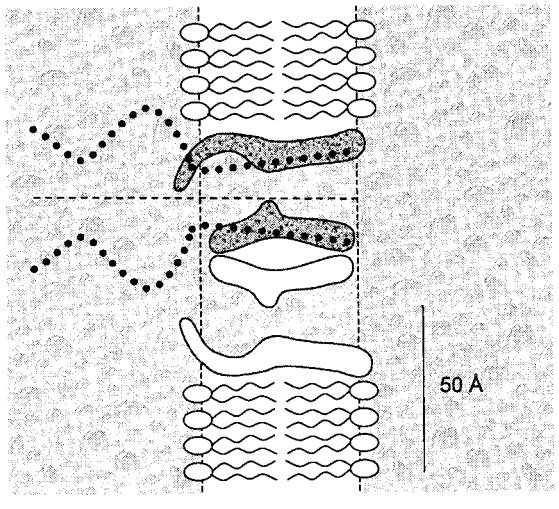

FIGURE 9 Pore geometries for OmpF porin (the grayish structure embedded in lipid bilayer) and α-toxin channel (dots extending to the membrane-bathing solution) deduced from crystallographic data (Cowan et al., 1992 and Dutzler et al., 1999; Song et al., 1996) differ significantly from that of the regular cylinder. By using Eq. 6 we introduce an effective pore radius to compare results on partitioning given in Fig. 8.

α-toxin pore is given by dotted lines (see also Merzlyak et al., 1999). It is seen that the shape of both pores is far from that of a regular simple cylinder. Their radii change with distance along the channel axis and, especially in the case of OmpF, the cross-sections are not even circular. To approximate these objects with a regular cylinder of radius R we introduce an effective radius by

$$R_{\text{eff}} = \left(\frac{\pi}{L} \int_0^L \frac{dz}{S(z)} \right)^{-1/2} \tag{6}$$

where $S(z)$ is the pore cross-section area at distance z from the channel opening and L is the channel length. This measure was chosen because all our results are based on conductance data, and it is clear that for a *macroscopic* pore with a smooth $S(z)$ function the value $\pi R_{\text{eff}}^2 \sigma / L$ (where σ is conductivity of the filling solution) equals pore conductance. Indeed, for a simple regular cylinder the effective radius coincides with the cylinder's radius, $R = R_{\text{eff}}$.

Using Eq. 6 and the pore structures (Cowan et al., 1992; Dutzler et al., 1999; Song et al., 1996) illustrated in Fig. 9 we obtain ~0.7 nm for the effective radius of the OmpF pore and ~1.0 nm for the α-toxin pore. Characteristic "cutoff" polymer molecular weights found for these channels in polymer partitioning experiments are $w_0^{\text{OmpF}} = 1360$ and $w_0^{\text{tox}} = 2200$ (Fig. 8). The ratio of corresponding polymer hydrodynamic radii, $(w_0^{\text{tox}}/w_0^{\text{OmpF}})^{0.6}$, is 1.3, which is close to the ratio of the effective channel radii calculated above: $1.0/0.7 = 1.4$. It is interesting to note here that the conductance of the OmpF monomeric pore is significantly *larger* than the conductance of the α-toxin channel (1.4 nS vs. 0.9 nS in 1 M KCl aqueous solutions). Therefore, without the knowledge of the crystal structure, which reveals a much longer pore for the α-toxin channel, the conclusion about the relative radii based on Ohm's law would be exactly opposite.

It is tempting to use the obtained effective radii to estimate conductance of OmpF and α-toxin channels by assigning bulk electrolyte conductivity (for our solutions, $\sigma = 10.5$ S/m at 23°C) to the water-filled region of their pores. Substituting the R_{eff} values for these channels into $\pi R_{\text{eff}}^2 \sigma / L$ and taking L equal to 4 nm and 10 nm, we get 4.0 nS and 3.3 nS for OmpF and α-toxin channels, correspondingly. This calculation does not include corrections from channel access resistances, but even with a 0.15 correction for the access resistance (see Fig. 4) these numbers are still about threefold higher than the actual channel conductance in both cases. Therefore, even for these large channels, their conductance, calculated using Ohm's law, is a poor measure of their pore size. The absence of a simple correlation between the channel pore size and the single-channel conductance was realized many years ago (Finkelstein, 1985). Recent studies confirm this observation and search for possible explanations (Smart et al., 1997; Tieleman and Berendsen, 1998; Phale et al., 2001).

Polymer mobility in the pore

The dynamics of polymer exchange between the pore and the bulk can be inferred from polymer-induced noise in the ion current through an open channel (Bezrukov et al., 1994). It was found that in both alamethicin and α-toxin channels PEG addition generates excess noise whose low-frequency spectral density is "white" (i.e., frequency-independent) at frequencies below several kHz. Plotted as a function of PEG molecular weight it reaches a maximum at molecular weights close to the corresponding "cutoff weight," w_0 (for a short review see Bezrukov and Kasianowicz, 2001). In the case of α-toxin, polymer-induced noise peaks to about an order of magnitude higher values than for alamethicin, suggesting strong PEG-pore interactions (Bezrukov et al., 1996).

Unlike alamethicin and α-toxin channels, where PEG-induced fluctuations are quite pronounced, the OmpF channel shows only small effects. PEGs of intermediate molecular weights increase the level of open channel conductance fluctuations (see Fig. 6, *squares*). However, the effect is not as large as for alamethicin in a state of comparable conductance (*triangles*). Small PEGs even decrease channel noise compared to its magnitude without polymer (*dashed horizontal line*).

Noise in polymer-free solutions significantly exceeds equilibrium noise (7×10^{-29} A^2/Hz) or shot-noise (1.4×10^{-28} A^2/Hz, assuming independent ion translocation) and is probably related to fast unresolved conformational "breathing" of the channel (Sigworth, 1985; Bezrukov and Winterhalter, 2000). The solid line shows the level of this noise as expected to be changed by polymer presence. We calculate it assuming that its spectral density is proportional to the current squared, which is reasonably to expect if the polymer-induced conductance reduction and conformational "breathing" are independent from each other (e.g., Neher and Stevens, 1977; DeFelice, 1981). It is seen that channel noise in the presence of the smallest polymer used in this study, PEG 200, is very close to the calculated level.

To estimate the polymer mobility within the channel, we use a formula describing open channel noise generated by equilibrium exchange of non-conducting particles between the channel pore and the bathing solution (Bezrukov et al., 1994, 2000a; Bezrukov, 2000). This formula is obtained for a long cylindrical pore of length L and relates particle diffusion coefficient inside the pore, D, with a low-frequency "white" part of the power spectral density of the current noise, $S_i(0)$:

$$D = \Delta g_s \langle \Delta g \rangle L^2 V^2 / 3 S_i(0) \qquad (7)$$

where V is applied transmembrane voltage, $\langle \Delta g \rangle$ is the polymer-induced average reduction of the pore conductance, and Δg_s is the change in the pore conductance due to the entrance of one polymer.

Geometry of the OmpF pore significantly deviates from that of a regular cylinder, so that Eq. 7 has to be applied with caution. Our calculations based on Eq. 6 demonstrate that >80% of the total channel resistance can be attributed to the constriction zone, whose length is ~2.0 nm only. Taking this value as an effective channel length, and assuming that for PEG 1000 channel occupancy by the polymer is close to one, we have $D_{PEG1000} \sim 10^{-11}$ m^2/s. This coefficient describing PEG diffusion inside the OmpF pore is about an order of magnitude smaller than the corresponding diffusion coefficient in the bulk. As it was discussed elsewhere (Bezrukov, 2000) the reduction in mobility of a particle inside the channel pore of a comparable size can be explained by the restricted diffusion considerations (Bean, 1972). However, because of the large relative error and complex pore geometry, our estimate is very crude. The only conclusion we derive from noise measurements is that our data are compatible with an order of magnitude reduction in polymer mobility.

Thus, neither partitioning of small polymers nor polymer dynamics inside the pore show any specific attraction between PEG and OmpF. In this respect the situation is very much different from that for the α-toxin pore in concentrated electrolytes, where strong interactions are evident in both PEG partitioning and dynamics (Bezrukov et al., 1996; Merzlyak et al., 1999; Bezrukov and Kasianowicz, 2001).

CONCLUSIONS

The qualitative picture of soft polymer partitioning into the OmpF channel pore is simple. Small polymers partition easily and decrease small-ion currents through the channel to approximately the same degree as they do currents in the bulk; sufficiently large polymers are excluded and do not interfere with the small-ion flow. However, PEG partitioning has a *sharper* dependence on polymer molecular weight than available entropic repulsion models predict. The hard-spheres, random-flight model, and scaling approach summarized in Fig. 7 describe a much smoother transition between regimes of exclusion and penetration. Similar sharp dependencies were previously reported for syringomycin E (Kaulin et al., 1998), alamethicin and, especially, for α-toxin channels. As recently discussed (Bezrukov and Kasianowicz, 2001) several possible complications arising from polydispersity of PEG samples (see also Berestovskii et al., 2000), non-ideality of concentrated polymer solutions (see also Cifra and Bleha, 2001), or deviation of the pore shape from a regular cylinder all lead to the opposite effect, i.e., to a *flattening* of the theoretical predictions. The reasons for this persistent discrepancy between theory and experiment for channels of different chemical composition and structure remain unclear.

However, comparison of the x-ray structural data for the α-toxin (Song et al., 1996) and OmpF (Cowan et al., 1992) channels shows that polymer weights corresponding to the

transition between regimes of polymer exclusion and penetration are in good accord with the relative channel sizes expressed as the average effective radii.

PEG-induced noise is small compared to that in alamethicin or α-toxin channels. This finding correlates with the structural features of the OmpF channel showing a short but pronounced constriction in the pore center. Polymer dynamics inside the channel pore inferred from noise analysis are consistent with the diffusion coefficient reduced by an order of magnitude relative to its value in the bulk.

We are grateful to Adrian Parsegian, Louis DeFelice, Sasha Berezhkovskii, and Don Rau for fruitful discussions and comments on this manuscript.

T.R. acknowledges the National Science Foundation award #9816788.

REFERENCES

Bean, C. P. 1972. The physics of porous membranes—neutral pores. *In* Membranes. G. Eisenman, editor. Marcel Dekker, New York. 1–54.

Bendat, J. S., and A. G. Piersol. 1986. Random Data: Analysis and Measurement Procedures. John Wiley, New York.

Benz, R., K. Janko, W. Boos, and P. Lauger. 1978. Formation of large, ion-permeable membrane channels by the matrix protein (porin) of *Escherichia coli*. *Biochim. Biophys. Acta.* 511:305–319.

Benz, R., K. Janko, and P. Lauger. 1979. Ion selectivity of pores formed by the matrix protein (porin) of *Escherichia coli*. *Biochim. Biophys. Acta.* 551:238–247.

Benz, R., A. Schmid, and R. E. Hancock. 1985. Ion selectivity of Gram-negative bacterial porins. *J. Bacteriol.* 162:722–727.

Berestovskii, G. N., V. I. Ternovskii, and A. A. Kataev. 2000. Allowing for polymer polydispersion as a necessary condition for determination of aqueous pore diameters in cells walls and membranes using polymers. *Biofizika.* 45:69–78 (in Russian); *Biophysics.* 45:63–72.

Berezhkovskii, A. M., S. M. Bezrukov, D. J. Bicout, and G. H. Weiss. 1999. The influence of polymer on the diffusion of a spherical tracer. *J. Chem. Phys.* 111:5641–5644.

Bezrukov, S. M. 2000. Ion channels as molecular Coulter counters to probe metabolite transport. *J. Membr. Biol.* 174:1–13.

Bezrukov, S. M., A. M. Berezhkovskii, M. A. Pustovoit, and A. Szabo. 2000a. Particle number fluctuations in a membrane channel. *J. Chem. Phys.* 113:8206–8211.

Bezrukov, S. M., and J. J. Kasianowicz. 1997. The charge state of an ion channel controls neutral polymer entry into its pore. *Eur. Biophys. J.* 26:471–476.

Bezrukov, S. M., and J. J. Kasianowicz. 2001. Dynamic partitioning of neutral polymers into a single ion channel. *In* Structure and Dynamics of Confined Polymers. J. J. Kasianowicz, M. S. Z. Kellermayer, and D. W. Deamer, editors. Kluwer Publishers, Dordrecht, The Netherlands. 93–106.

Bezrukov, S. M., L. Kullman, and M. Winterhalter. 2000b. Probing sugar translocation through maltoporin at the single channel level. *FEBS Lett.* 476:224–228.

Bezrukov, S. M., and I. Vodyanoy. 1993. Probing alamethicin channels with water-soluble polymers. *Biophys. J.* 64:16–25.

Bezrukov, S. M., I. Vodyanoy, R. A. Brutyan, and J. J. Kasianowicz. 1996. Dynamics and free energy of polymers partitioning into a nanoscale pore. *Macromolecules.* 29:8517–8522.

Bezrukov, S. M., I. Vodyanoy, and V. A. Parsegian. 1994. Counting polymers moving through a single ion channel. *Nature.* 370:279–281.

Bezrukov, S. M., and M. Winterhalter. 2000. Examining noise sources at the single-molecule level: 1/*f* noise of an open maltoporin channel. *Phys. Rev. Lett.* 85:202–205.

Buehler, L. K., S. Kusumoto, H. Zhang, and J. P. Rosenbusch. 1991. Plasticity of *Escherichia coli* porin channels. Dependence of their conductance on strain and lipid environment. *J. Biol. Chem.* 266: 24446–24450.

Bullock, J. O., and E. R. Kolen. 1995. Ion selectivity of colicin E1. III. Anion permeability. *J. Membr. Biol.* 144:131–145.

Cafiso, D. S. 1994. Alamethicin: a peptide model for voltage gating and protein-membrane interactions. *Annu. Rev. Biophys. Biomol. Struct.* 23:141–165.

Casassa, E. F. 1967. Equilibrium distribution of flexible polymer chains between a macroscopic solution phase and small voids. *Polymer Lett.* 5:773–778.

Cifra, P., and T. Bleha. 2001. Partition coefficients and the free energy of confinement from simulations of nonideal polymer systems. *Macromolecules.* 34:605–613.

Colton, C. K., C. N. Satterfield, and C.-J. Lai. 1975. Diffusion and partitioning of macromolecules within finely porous glass. *ALChE J.* 21:289–298.

Couper, A., and R. F. T. Stepto. 1969. Diffusion of low-molecular weight poly(ethylene oxide) in water. *Trans. Faraday Soc.* 65:2486–2496.

Cowan, S. W. 1993. Bacterial porins: lessons from three high-resolution structures. *Curr. Opin. Struct. Biol.* 3:501–507.

Cowan, S. W., T. Schirmer, G. Rummel, M. Steiert, R. Ghosh, R. A. Pauptit, J. N. Jansonius, and J. P. Rosenbusch. 1992. Crystal structures explain functional properties of two *E. coli* porins. *Nature.* 358:727–733.

Decad, G. M., and H. Nikaido. 1976. Outer membrane of Gram-negative bacteria. XII. Molecular-sieving function of cell wall. *J. Bacteriol.* 128:325–336.

DeFelice, L. J. 1981. Introduction to Membrane Noise. Plenum Press, New York.

De Gennes, P.-G. 1979. Scaling Concepts in Polymer Physics. Cornell University Press, Ithaca, New York.

Desai, S. A., and R. L. Rosenberg. 1997. Pore size of the malaria parasite's nutrient channel. *Proc. Natl. Acad. Sci. USA.* 94:2045–2049.

Douglas, J. T., E. Y. Rosenberg, H. Nikaido, D. R. Verstreate, and A. J. Winter. 1984. Porins of Brucella species. *Infect. Immun.* 44:16–21.

Dutzler, R., G. Rummel, S. Alberti, S. Hernandez-Alles, P. Phale, J. Rosenbusch, V. Benedi, and T. Schirmer. 1999. Crystal structure and functional characterization of OmpK36, the osmoporin of *Klebsiella pneumoniae*. *Structure Fold Des.* 7:425–434.

Engel, A., A. Massalski, H. Schindler, D. L. Dorset, and J. P. Rosenbusch. 1985. Porin channel triplets merge into single outlets in *Escherichia coli* outer membranes. *Nature.* 317:643–645.

Finkelstein, A. 1985. The ubiquitous presence of channels with wide lumens and their gating by voltage. *Ann. N.Y. Acad. Sci.* 456:26–32.

Grosberg, A. Yu., and A. R. Khokhlov. 1994. Statistical Physics of Macromolecules. AIP Press, New York.

Howorka, S., L. Movileanu, X. F. Lu, M. Magnon, S. Cheley, O. Braha, and H. Bayley. 2000. A protein pore with a single polymer chain tethered within the lumen. *J. Am. Chem. Soc.* 122:2411–2416.

Kaulin, Yu. A., L. V. Schagina, S. M. Bezrukov, V. V. Malev, A. M. Feigin, J. Y. Takemoto, J. H. Teeter, and J. G. Brand. 1998. Cluster organization of ion channels formed by the antibiotic syringomycin E in bilayer lipid membranes. *Biophys. J.* 74:2918–2925.

Korchev, Yu. E., C. L. Bashford, G. M. Alder, J. J. Kasianowicz, and C. A. Pasternak. 1995. Low conductance states of a single ion channel are not "closed." *J. Membr. Biol.* 147:233–239.

Krasilnikov, O. V. 2001. Sizing channels with polymers. *In* Structure and Dynamics of Confined Polymers. J. J. Kasianowicz, M. S. Z. Kellermayer, and D. W. Deamer, editors. Kluwer Publishers, Dordrecht, The Netherlands. 73–91.

Krasilnikov, O. V., J. B. Da Cruz, L. N. Yuldasheva, and R. A. Nogueira. 1998. A novel approach to study the geometry of the water lumen of ion channels: colicin Ia channels in planar lipid bilayers. *J. Membr. Biol.* 161:83–92.

Krasilnikov, O. V., R. Z. Sabirov, V. I. Ternovsky, P. G. Merzlyak, and J. N. Muratkhodjaev. 1992. A simple method for the determination of

the pore radius of ion channels in a planar lipid bilayer membrane. *FEMS Microbiol. Immunol.* 5:93–100.

Kuga, S. 1981. Pore size distribution analysis of gel substances by size exclusion chromatography. *J. Chromatogr.* 206:449–461.

Lou, K.-L., N. Saint, A. Prilipov, G. Rummel, S. A. Benson, J. P. Rosenbusch, and T. Schirmer. 1996. Structural and functional characterization of OmpF mutants selected for larger pore size. I. Crystallographic analysis. *J. Biol. Chem.* 271:20669–20675.

Merzlyak, P. G., L. N. Yuldasheva, C. G. Rodrigues, C. M. M. Carneiro, O. V. Krasilnikov, and S. M. Bezrukov. 1999. Polymeric nonelectrolytes to probe pore geometry: application to the α-toxin transmembrane channel. *Biophys. J.* 77:3023–3033.

Montal, M., and P. Mueller. 1972. Formation of biomolecular membranes from lipid monolayers and study of their electrical properties. *Proc. Natl. Acad. Sci. U.S.A.* 69:3561–3566.

Movileanu, L., S. Cheley, S. Howorka, O. Braha, and H. Bayley. 2001. Location of a constriction in the lumen of a transmembrane pore by targeted covalent attachment of polymer molecules. *J. Gen. Physiol.* 117:239–251.

Nakae, T. 1976a. Identification of the outer membrane protein of *E. coli* that produces transmembrane channels in reconstituted vesicle membranes. *Biochem. Biophys. Res. Commun.* 71:877–884.

Nakae, T. 1976b. Outer membrane of Salmonella. Isolation of protein complex that produces transmembrane channels. *J. Biol. Chem.* 251: 2176–2178.

Neher, E., and C. F. Stevens. 1977. Conductance fluctuations and ionic pores in membranes. *Annu. Rev. Biophys. Bioeng.* 6:345–381.

Nikaido, H., and E. Y. Rosenberg. 1983. Porin channels in *Escherichia coli*: studies with liposomes reconstituted from purified proteins. *J. Bacteriol.* 153:241–252.

Nikaido, H., and M. Vaara. 1985. Molecular basis of bacterial outer membrane permeability. *Microbiol. Rev.* 49:1–32.

Parsegian, V. A., S. M. Bezrukov, and I. Vodyanoy. 1995. Watching small molecules move: interrogating ionic channels using neutral solutes. *Biosci. Rep.* 15:503–514.

Phale, P. S., A. Philippsen, C. Widmer, V. P. Phale, J. P. Rosenbusch, and T. Schirmer. 2001. Role of charged residues at the OmpF porin channel constriction probed by mutagenesis and simulation. *Biochemistry.* 40: 6319–6325.

Saint, N., K.-L. Lou, C. Widmer, M. Luckey, T. Schirmer, and J. P. Rosenbusch. 1996. Structural and functional characterization of OmpF porin mutants selected for larger pore size. II. Functional characterization. *J. Biol. Chem.* 271:20676–20680.

Sansom, M. S. P. 1991. The biophysics of peptide models of ion channels. *Prog. Biophys. Mol. Biol.* 55:139–235.

Schindler, H., and J. P. Rosenbusch. 1978. Matrix protein from *Escherichia coli* outer membranes forms voltage-controlled channels in lipid bilayers. *Proc. Natl. Acad. Sci. U.S.A.* 75:3751–3755.

Sigworth, F. J. 1985. Open channel noise. I. Noise in acetylcholine receptor currents suggests conformational fluctuations. *Biophys. J.* 47:709–720.

Smart, O. S., J. Breed, G. R. Smith, and M. S. P. Sansom. 1997. A novel method for structure-based prediction of ion channel conductance properties. *Biophys. J.* 72:1109–1126.

Song, L., M. R. Hobaugh, C. Shustak, S. Cheley, H. Bayley, and J. E. Gouaux. 1996. Structure of staphylococcal α-hemolysin, a heptameric transmembrane pore. *Science.* 274:1859–1865.

Ternovsky, V. I., and G. N. Berestovsky. 1998. Effective diameter and structural organization of reconstituted calcium channels from the Characeae algae Nitellopsis. *Membr. Cell Biol.* 12:79–88.

Tieleman, D. P., and H. J. C. Berendsen. 1998. A molecular dynamics study of the pores formed by *Escherichia coli* OmpF porin in a fully hydrated palmitoyloleoylphosphatidylcholine bilayer. *Biophys. J.* 74: 2786–2801.

Villarroel, A., N. Burnashev, and B. Sakmann. 1995. Dimensions of the narrow portion of the recombinant NMDA receptor channel. *Biophys. J.* 68:866–875.

Wallace, B. A. 2000. Common structural features in gramicidin and other ion channels. *Bioessays.* 22:227–234.

Zimmerberg, J., and V. A. Parsegian. 1986. Polymer inaccessible volume changes during opening and closing of a voltage-dependent ion channel. *Nature.* 323:36–39.